Investigations of the opto-dielectric effects in the vicinity of the smectic-A–smectic-C_A^* transition

2006 J. Phys.: Condens. Matter 18 9415

(http://iopscience.iop.org/0953-8984/18/41/008)

INSTITUTE OF PHYSICS PUBLISHING JOURNAL OF PHYSICS: CONDENSED MATTER

J. Phys.: Condens. Matter **18** (2006) 9415–9425 doi:10.1088/0953-8984/18/41/008

Investigations of the opto-dielectric effects in the vicinity of the smectic-A–smectic-C^*_A transition

Geetha G Nair[1], Gurumurthy Hegde[1], S Krishna Prasad[1] and Y S Negi[2]

[1] Centre for Liquid Crystal Research, Jalahalli, Bangalore 560 013, India
[2] Centre for Materials for Electronics Technology, Panchwati, Off Pashan Road, Pune 411 008, India

Received 4 May 2006, in final form 23 August 2006
Published 29 September 2006
Online at stacks.iop.org/JPhysCM/18/9415

Abstract

Dielectric investigations of the photoinduced effects in the vicinity of the smectic A (Sm-A)–antiferroelectric smectic C (Sm-C^*_A) transition of a guest–host system consisting of photoactive azobenzene-based guest molecules and non-photoactive host molecules have been carried out. The frequency-dependent dielectric data is analysed in terms of a molecular mode and a high-frequency mode. We observe that the dielectric parameters associated with the two modes show primary as well as secondary photoferroelectric effects, in agreement with the effects observed in our previous study (Nair *et al* 2006 *Phys. Rev.* E **73** 011712, referred to as [1] in the present article) for polarization and response time. Here the primary photoelectric effect is associated with changes in the polar ordering and/or transverse molecular dipole moment at a constant reduced temperature and the secondary effect is due to the radiation-induced reduction in the transition temperature. The temporal variation of the relaxation parameters shows that the photoinduced isothermal transition as well the thermal back relaxation occurs on fast timescales.

1. Introduction

Since the discovery of antiferroelectricity [2] in liquid crystals, a number of materials exhibiting the antiferroelectric Sm-C^* or Sm-C^*_A phase have been reported. In the Sm-C^*_A phase the molecules in the neighbouring layers are tilted from the smectic layer normal in almost opposite directions. Generally, the Sm-C^* phase intervenes between the Sm-A and Sm-C^*_A phases and systems with a direct transition from the Sm-A to the Sm-C^*_A phase are rare [3]. A particular aspect of the Sm-C^*_A phase that has been well debated is its dielectric property, especially the relaxation modes it exhibits.

The phenomenon of reversible shape transformation of chromophoric molecules, such as azobenzenes, driven by photo-induced isomerization has been extensively studied [4]. The principle behind the phenomenon is outlined in the following. Upon UV irradiation (around

360 nm, corresponding to the π–π^* band of the azo group), the energetically more stable *E* configuration with an elongated rod-like molecular form changes into the bent *Z* configuration. The reverse transformation can be brought about by illuminating with visible light (around 450 nm, corresponding to the n–π^* band). This latter change can also occur spontaneously in the 'dark' by a process known as *thermal back-relaxation*. The liquid crystalline phase is stabilized by the rod-like *E* form, but is destabilized by the bent *Z* form. The *E*–*Z* (or trans–cis) conformational change of the azobenzene molecules, present as guest molecules in a guest–host environment of host liquid crystalline material, can result in a photoinduced isothermal transition, a feature that has been observed for a variety of systems exhibiting different phases [5–17]. Our earlier paper [1] describes detailed measurements of the photoinduced effects on the electric polarization, tilt angle, response time and rotational viscosity in the vicinity of the smectic A (Sm-A)–antiferroelectric smectic C (Sm-C_A^*) transition of a guest–host system consisting of photoactive azobenzene-based guest molecules and non-photoactive host molecules. In this paper we report the effect of light on the dielectric properties in the vicinity of the Sm-A–Sm-C_A^* transition of the same system.

2. Experimental details

The compound 4-(1-trifluoromethylheptyloxy carbonyl) phenyl 4′-octyloxybiphenyl 4-carboxylate (TFMHPOBC for short), originally synthesized by Suzuki *et al* [18], and exhibiting the Sm-A–Sm C_A^* transition, was used as the host and the photoactive guest compound was 4-(4-ethoxyphenylazo)phenyl hexanoate (EPH for short) having a nematic mesophase. The molecular structures of these two compounds are shown below.

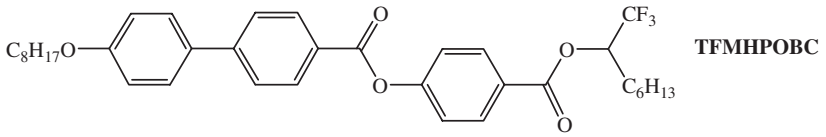

TFMHPOBC

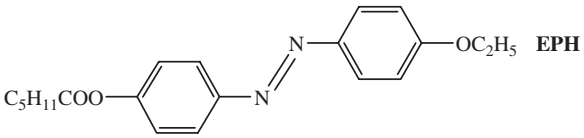

EPH

All the measurements reported in this paper have been carried out on a mixture (referred to as mixture 1 hereafter) containing 5%, by weight, of EPH in TFMHPOBC. Polarizing microscopy observations showed that mixture 1 exhibits the sequence isotropic (Iso)–Sm-A–Sm-C_A^*.

The UV apparatus used for inducing photo-isomerization consisted of an intensity-stabilized UV source with a fibre-optic guide (Hamamatsu L7212-01, Japan) along with a UV-band pass filter (UG 11, Newport). An additional IR-block filter was inserted just before the sample to prevent any effects of heat radiation from the UV source. The actual power (I_{UV}) of the radiation passing through the filter combination falling on the sample was measured with a UV power meter (Hamamatsu, C6080-03) kept in the sample position. The variation of the intensity monitored over a typical experimental duration ($\sim$1 h) was found to be less than 0.01 mW cm^{-2}. The dielectric measurements were carried out by measuring the capacitance of the sample using an impedance analyser (HP 4194A). With a user-written program we were able to collect an entire frequency sweep from 100 Hz to 10 MHz in less than 5 s, a feature extremely useful to perform time-resolved dielectric dispersion measurements. The dielectric studies were carried out in two different geometries: homeotropic and planar.

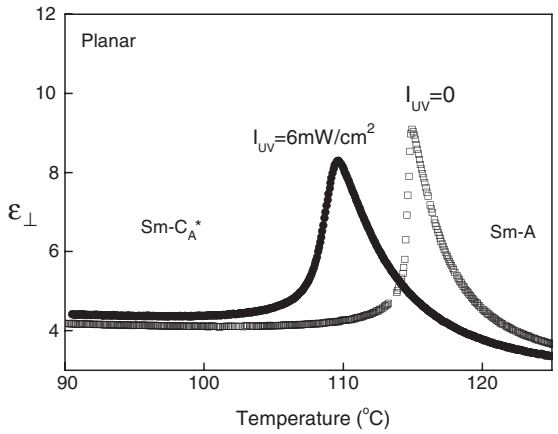

Figure 1. Thermal variation of the dielectric constant in the vicinity of the Sm-A–Sm-C_A^* transition measured at a frequency of 1 kHz in planar geometry ($\varepsilon_\perp$) with no UV and for UV power $I_{UV} = 6$ mW cm^{-2}. Since the phase does not possess a 'true' Goldstone mode the $\varepsilon_\perp$ value peaks at the transition, suggesting a soft mode contribution to the dielectric constant. The error in the measurement of the dielectric constant is much smaller than the dimension of the data markers used.

The homeotropic orientation of the molecules was obtained by treating the glass substrate surface with a silane solution and the planar geometry was realized by depositing a layer of polyimide on the substrate surface. In both situations a very good alignment of the molecules was observed and thus the dielectric constants measured correspond to that parallel ($\varepsilon_\parallel$—homeotropic geometry) and perpendicular ($\varepsilon_\perp$—planar geometry) to the director in the Sm-A phase. The sheet resistance of indium tin oxide coating on the glass plates was only a few ohms. This feature in combination with the fact that the dielectric constant is low in all the phases of mixture 1 allowed studies to be performed in the MHz region. For the temperature-dependent experiments, the temperature of the sample, placed inside a hot-stage (Mettler FP82 HT) controlled by a microprocessor (Mettler FP90), was ramped at a rate of 1 K min^{-1}, resulting in a variation of $<$100 mK (measured with a precision of 10 mK) during any frequency scan. For the temporal scans the temperature was kept constant to within 0.1 K.

3. Results and discussion

3.1. Temperature-dependent measurements

The temperature dependence of the dielectric constant $\varepsilon_\perp$ obtained in planar geometry at a fixed frequency of 1 kHz is shown in figure 1 with no UV and for $I_{UV} = 6$ mW cm^{-2}. The peaking of $\varepsilon_\perp$ at the Sm-A–Sm-C_A^* transition [19] as well as the decrease in the transition temperature T_c, when the sample is illuminated with UV are known features [5–17]. Another feature that is observed in figure 1 is that when UV radiation is present the transition region becomes broad. From a simple point of view the diminution in the transition temperature and the broadening of the transition upon creation of bent Z isomers can be thought of as being similar to the impurity-determined behaviour in binary systems.

Figure 2 shows the representative ε'' (the imaginary part of the dielectric constant) versus frequency scans obtained in the Sm-A and Sm-C_A^* phases. To extract the relaxation parameters (frequency f_R and dielectric strength $\Delta\varepsilon_R$) the data were fitted to the Havriliak–Negami (HN)

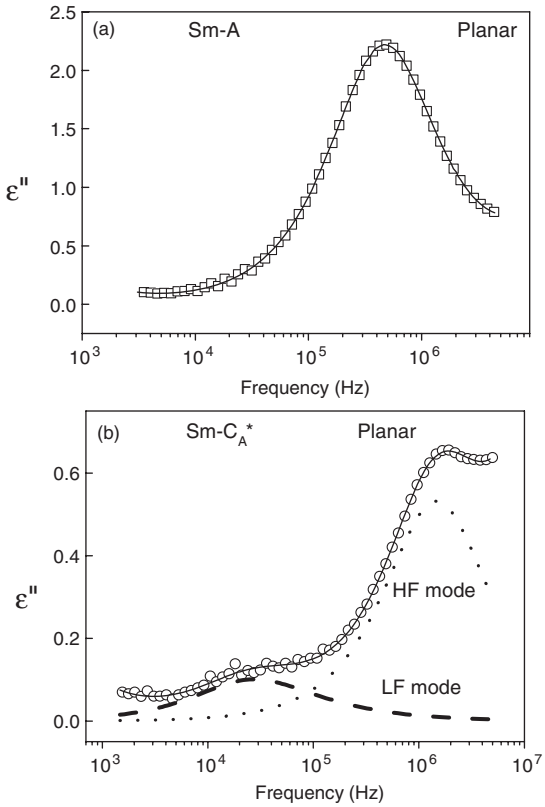

Figure 2. Frequency dependence of ε'' in planar geometry for the (a) Sm-A and (b) Sm-C_A^* phases. The solid line through the points shows the best fit to the HN equation. In the Sm-A phase only one relaxation is seen whereas the data in the Sm-C_A^* show two relaxations: the resolved data are shown as the low-frequency (LF) mode (dashed line) and the high-frequency (HF) mode (dotted line). Typical α and β values are 0.94 and 0.83 for the LF mode, and 0.97 and 1.0 for the HF mode respectively. The error in the determination of the relaxation frequency and strength is ∼3% for the HF mode and 5% for the LF mode.

equation [20].

$$\varepsilon^*(f) = \mathrm{i}\sigma(f) + \varepsilon_\infty + \frac{\Delta\varepsilon_\mathrm{R}}{[1 + (\mathrm{i}f/f_\mathrm{R})^\alpha]^\beta}. \tag{1}$$

Here f is the measuring frequency, ε_∞ is the sum of the dielectric strengths of all the high-frequency modes other than the one under consideration. $\Delta\varepsilon_\mathrm{R}$ is the difference between low- and high-frequency dielectric constants and is a measure of the dielectric strength of the mode of interest, and f_R is the characteristic relaxation frequency. The parameters α and β describe the width and asymmetric broadening of the relaxation curve; $\alpha = 1$ and $\beta = 1$ represent a Debye curve. To account for the DC conductivity (σ) contribution to the imaginary part of the dielectric constant, the term $\mathrm{i}\sigma(f)$ was needed.

While in the Sm-A phase only one relaxation mode is observed, in the Sm-C_A^* phase two modes are seen. In the Sm-A phase the assignment of the mode is unambiguous, arising from the softening of the tilt fluctuations, and therefore we refer to it as the soft mode. In contrast, regarding the assignment of the modes observed in the Sm-C_A^* phase, there has been confusion and much debate [21–27], and therefore we will refer to them merely as low-frequency (LF)

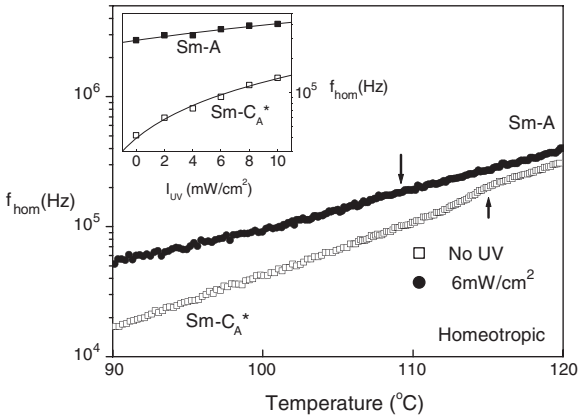

Figure 3. Thermal variation of the relaxation frequency of the molecular mode for no UV and $I_{UV} = 6$ mW cm^{-2} showing the primary photoferroelectric effect in the relaxation behaviour of the molecular mode. (The typical α and β values for this mode are 0.98 and 1.0, and the error in the determination of the relaxation frequency and strength is ∼1%.) In the Sm-A phase (119 °C) the data for no UV and $I_{UV} = 6$ mW cm^{-2} almost coincide whereas deep in the Sm-C$^*_A$ phase (100 °C) the value is much higher for the data set with UV. The inset shows the UV-induced enhancement of f_{hom} as a function of I_{UV} with a significant increase in the Sm-C$^*_A$ phase (open squares), but only a small change in the Sm-A phase (filled squares). The arrows indicate the transition temperatures as determined from the data for the HF mode.

mode with a corresponding frequency f_2 and high-frequency (HF) mode with a corresponding frequency of f_1. It may, however, be mentioned that since the relaxation mode seen with homeotropic geometry (with a corresponding frequency f_{hom}) has nearly the same relaxation frequency as the LF mode although with a factor of 4 larger dielectric strength, we tend to think that the LF mode is the molecular mode associated with the rotation of the molecules around the short axis. At all the temperatures investigated, while the HF mode and that seen in the homeotropic geometry were found to be nearly Debye-type relaxations with $\alpha = 0.97$, $\beta = 1$ and $\alpha = 0.98$ and $\beta = 0.9$ respectively, the LF mode was seen to be having a slight asymmetric distribution with a value of $\beta \sim 0.8$, but still having a narrow distribution function with $\alpha \sim 0.97$.

The thermal variation of the relaxation frequency of the molecular mode (f_{hom}) is shown in figure 3 for the no-UV and $I_{UV} = 6$ mW cm^{-2} cases. The feature to be noted is that, at the transition, f_{hom} has an abrupt change for the no-UV case, but a gradual variation for the UV case. Another point to be noted in figure 3 is that the f_{hom} values for the two sets appear to converge in the high-temperature region of the Sm-A phase, whereas in the Sm-C$^*_A$ phase the value is definitely higher for the UV case. The inset to figure 3 shows the different behaviour of the f_{hom} values at temperatures deep in the two phases as a function of I_{UV}: while the Sm-A value shows a small increase (290–410 kHz, i.e., 40%) even for $I_{UV} = 10$ mW cm^{-2}, the value in the Sm-C$^*_A$ phase has a substantial increase (42–134.5 kHz, i.e., 220%) for the same power. As discussed in [1], the influence of light can be separated into primary and secondary effects. The latter causes a change in the property under consideration owing to a shift in the transition temperature. The primary effect, on the other hand, is due to a change in the polar ordering and/or the transverse dipole moment. We see both the effects in the data shown in figure 3. While the secondary effect is obvious (T_c shifts by as much as 5 °C for $I_{UV} = 6$ mW cm^{-2}), the inset to figure 3 clearly demonstrates that the primary effect is also significant, with f_{hom} becoming more than double in the Sm-C$^*_A$ phase upon UV illumination.

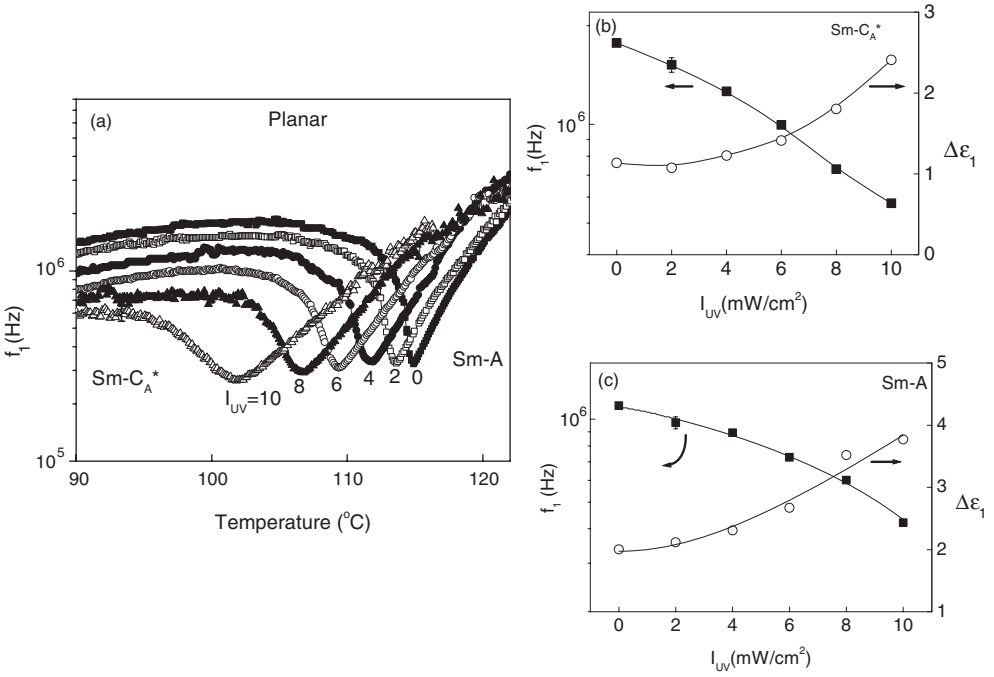

Figure 4. (a) Temperature dependence of the relaxation frequency f_1 (HF mode) without UV illumination and for various values of I_{UV} (in mW cm^{-2}). In each case the softening of the mode on approaching the transition from the Sm-A side is clearly seen with the minimum at T_c. In the Sm-A phase, like in the case of molecular mode, away from the transition f_1 values seem to converge, whereas in Sm-C$_A^*$ there is substantial decrease with UV illumination unlike for the molecular mode. The UV intensity dependence of the saturated values of the relaxation parameters f_1 and $\Delta\varepsilon_1$ in (b) Sm-C$_A^*$ phase at $T_c - 10\,^\circ$C and in (c) Sm-A phase at $T_c + 4\,^\circ$C. The error in the determination of the two parameters was $\sim$3%.

If this is indeed the molecular mode connected with the reorientation of the molecules about their short axis, then the increase in f_{hom} upon illumination could be due to the following argument. In the case of a photoactive liquid crystal exhibiting the nematic phase, we have found that photoisomerization of the system results in a substantial increase in the relaxation frequency associated with the reorientation of the molecules about the short axis [28]. In such systems the UV illumination and the formation of the bent Z isomers leads to a reduction in the nematic orientational order parameter, consequently increasing the relaxation frequency. A similar effect happening in the present system causing the frequency of the molecular mode to increase upon UV illumination should not be surprising. Using the slope of the f_{hom} versus temperature behaviour the activation energy was calculated. In the absence of UV illumination the activation energy values are similar, 110 and 105 kJ mol^{-1}, in the Sm-A and Sm-C$_A^*$ phases. The values decrease for $I_{UV} = 6$ mW cm^{-2}, yielding 93 and 66 kJ mol^{-1} in the Sm-A and Sm-C$_A^*$ phases, with the change being more drastic for the tilted phase.

The influence of UV illumination on the temperature dependence of the HF relaxation frequency f_1 is shown in figure 4(a). The softening nature of the mode in the Sm-A phase is clear at all I_{UV} values. Quite similar to the data for the molecular mode in the Sm-A phase, away from the transition the f_1 values seem to converge to a point, whereas in the Sm-C$_A^*$ phase there is a substantial decrease when UV radiation is shone, unlike for the molecular mode. To illustrate this point we show in figures 4(b) and (c) the f_1 and $\Delta\varepsilon_1$ values obtained at a constant

reduced temperature of $T_c - 10\,^{\circ}$C (Sm-C_A^*) and $T_c + 4\,^{\circ}$C (Sm-A) as a function of I_{UV}. In both phases f_1 and $\Delta\varepsilon_1$ show a nonlinear variation as I_{UV} increases, with f_1 coming down from 1.8 MHz to 575 kHz in the Sm-C_A^* phase and 1.1 MHz to 430 kHz in the Sm-A phase for no UV and $I_{UV} = 10$ mW cm^{-2} respectively. The $\Delta\varepsilon_1$ value, on the other hand, increases by a factor of 2 between the two conditions for both phases. A point that should be emphasized is that, as discussed earlier, while the assignment of the relaxation mode is not very clear in the Sm-C_A^* phase, it is unambiguously the soft mode in the Sm-A phase. With this in mind we look at the data in the Sm-A phase in terms of the mean field model that considers the softening of the mode on approaching the transition from the Sm-A phase to a tilted smectic. According to the mean-field model [29, 30], the temperature dependence of the soft mode parameters $\Delta\varepsilon_1$ and f_1 can be expressed as

$$f_1 = \frac{1}{2\pi\eta}(a(T - T_c) + Kq_0^2) \tag{2}$$

$$\Delta\varepsilon_1 = \frac{\varepsilon_0(\varepsilon C)^2}{Kq_0^2 + a(T - T_c)}. \tag{3}$$

Here K is an elastic term, related to the bend elastic constant K_3, q_0 is the wavevector corresponding to the helical pitch of the low-temperature tilted smectic phase, η is the viscosity associated with the mode, and ε and ε_0 are the high-frequency and free space permittivities, respectively. C is a coefficient representing the linear coupling between polarization and tilt angle and a is the usual Landau coefficient associated with the square of the order parameter. A full analysis of the data using equations (2) and (3) requires the parameters a, K, q_0 and η. To simplify matters we consider the product

$$\frac{1}{\Delta\varepsilon_1 f_1} = \frac{2\pi\eta}{\varepsilon_0(\varepsilon C)^2}. \tag{4}$$

This equation has the advantage that if C, the chiral coupling coefficient, is known, the soft-mode viscosity can be calculated. The value of C has been determined in an earlier study [1] using polarization and tilt angle data collected in the Sm-C_A^* phase for the no-UV and $I_{UV} = 4$ mW cm^{-2} conditions to be 4.4×10^7 and 5.2×10^7 V m^{-1} respectively. Substituting these values gives η as 30.5 and 46.1 mPa s for the no-UV and UV conditions at $T_c + 4\,^{\circ}$C. The 50% increase in the tilt mode viscosity in the presence of the UV radiation causes the significant slowing down of the soft mode when the sample is illuminated. This feature is interesting since in combination with the enhanced C value it would result in a higher electroclinic tilt angle.

3.2. Temporal measurements

Figure 5 shows representative dielectric absorption (ε'') scans taken at a temperature ($T_c - 1.6\,^{\circ}$C, i.e., in the Sm-C_A^* phase) in the absence of UV light and at $t = 7$, 13, 19, 40 and 157 s time intervals after turning it on ($I_{UV} = 4$ mW cm^{-2}) and at $t = 90$ s after turning it off. The drastic change in the relaxation parameters upon UV illumination is evident from this diagram. It must be emphasized that when the radiation is turned off, the system recovers the original peak (compare the scans labelled as before UV on and after UV off). As was done for the temperature-dependent measurements, ε'' versus frequency data were fitted to the HN expression. At all UV intensities used in this study, the profiles were close to the ideal Debye type of relaxation. The temporal variation of $\Delta\varepsilon_1$ at a reduced temperature of $T_c - 5\,^{\circ}$C and with a UV power of 4 mW cm^{-2} is shown in figure 6. (Generally, the kinetics of the UV on/off process can be analysed in terms of two timescales: delay time and response time. The former is defined as the duration between the instant of radiation on/off and the instance at which the sample response begins. Once begun, the sample takes a finite duration, termed the

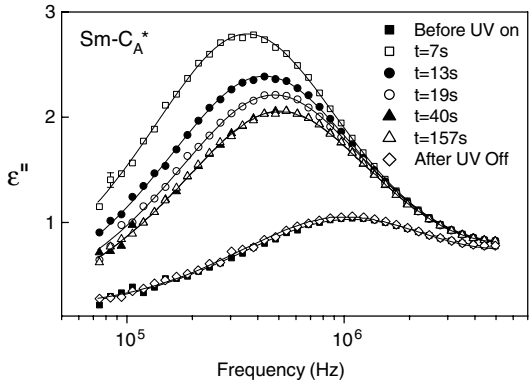

Figure 5. Dielectric absorption spectra taken in the Sm-C_A^* phase (1.6 °C below the transition), obtained before ($t = 0$ s) and at $t = 7$, 13, 19, 40 and 157 s after the UV illumination of power 4 mW cm^{-2} is turned on and at $t = 90$ s after switching the UV illumination off. The last of these data sets overlaps very well with that measured before shining the UV radiation, again proving the reproducible nature of the phenomenon. The response of the system reaches a limit after a certain duration of the UV illumination being on, as can be seen by the data sets at $t = 40$ and 157 s. The solid lines represent the fit to the HN equation.

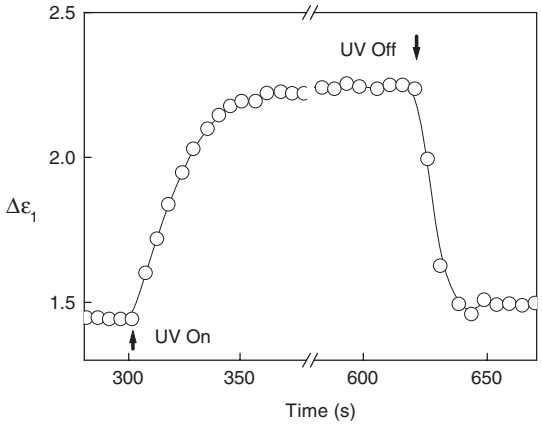

Figure 6. Time-dependent variation of the dielectric strength of the HF mode at a reduced temperature of $T_c - 5$ °C upon turning the UV illumination on and subsequently off. The error in the determination of $\Delta\varepsilon_1$ was 3%.

response time, to complete the process.) Several features seen here are interesting. The change in $\Delta\varepsilon_1$ during both the UV-on and the thermal back-relaxation processes takes place without any measurable delay. This situation, particularly for the latter process, is different from that for the nematic–isotropic (N–Iso) transition where the recovery of the original state is always associated with a substantial delay time after the UV light is switched off. The second feature to be noticed is that the response time involved for the process to take place is comparable (∼20 s) for both the UV-on and UV-off conditions, again in contrast to that for the N–Iso case, where the back-relaxation is always at least an order of magnitude slower than the on process. It is also observed that the data for the UV-on process follows a first-order kinetics whereas the UV-off process is faster than that. A possible reason why the dynamics is faster in the present case compared to that for the N–Iso transition could be that here the transition involves

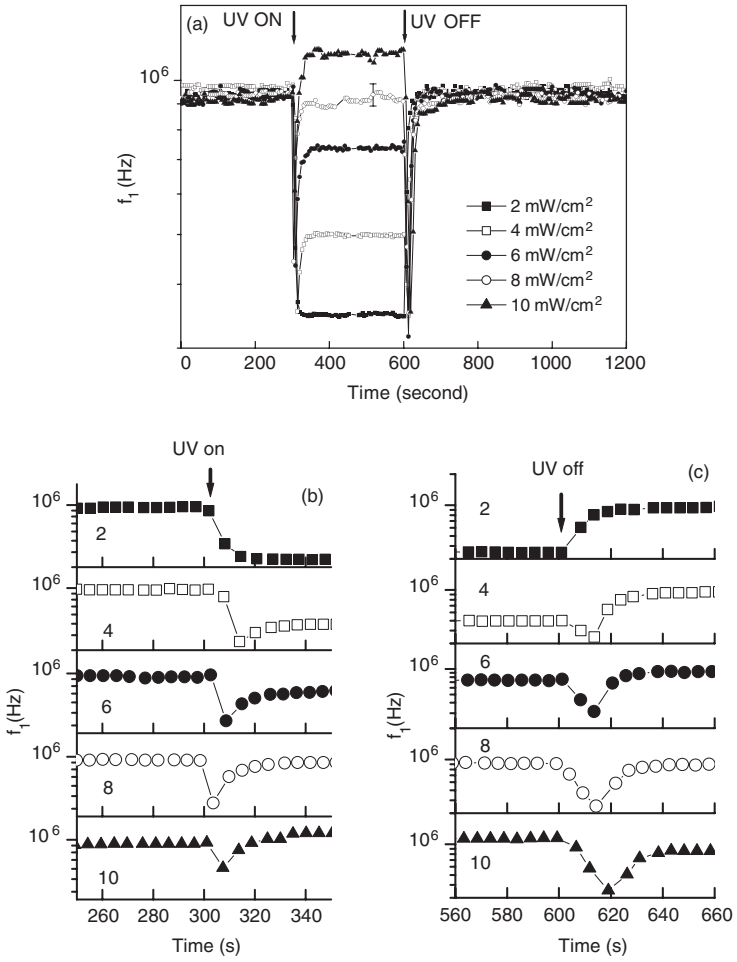

Figure 7. (a) The effect of the magnitude of the UV illumination on the time-resolved variation of the relaxation frequency f_1. To bring out the details of the photoinduced and the thermal back relaxation process, the data in the vicinity of the UV light on and off sequences are shown on an enlarged scale in (b) and (c) respectively. The instants at which the UV radiation was turned on and subsequently off are marked with downward pointing arrows. (Throughout these measurements the sample was maintained at a temperature of 1.6 °C below T_c of the unirradiated sample.)

a layered phase, with a much larger orientational order than in the N phase and of course it has the additional layering order. Owing to the better ordering the system does not tolerate large changes in the ordering (that is brought about by the shape changes in the azobenzene molecule) unless there is a driving force like the UV radiation. Hence when the radiation is switched off the system will recover its original state quickly.

The temporal variation of f_1 upon illuminating the sample with UV radiation of different I_{UV} values at a constant temperature of 1.6 °C below T_c of the unirradiated sample are shown in figure 7(a); the time regions close to the photoinduced transition and the thermal back-relaxation are shown on an enlarged timescale in figures 7(b) and (c) respectively. It is observed that this overall change takes place in 40–60 s before attaining the photostationary state. When the radiation is switched off, the reverse phenomenon takes place and most importantly the

system recovers the original values that existed before UV irradiation. The qualitative variation of f_1 with time is not the same at all UV intensities. For $I_{UV} = 2$ mW cm^{-2} the value of f_1 decreases monotonically with time after the UV light is turned on. For higher I_{UV} values, f_1 decreases immediately after turning the radiation on, but reverses its trend after a certain time interval. Comparing this data with the temperature dependence of these parameters, one notices that such a reversal in the trend signifies that the Sm-A–Sm-C$^*_A$ transition has taken place, albeit photoinduced and isothermal, and that I_C, the critical intensity to bring about the phase transition, lies in the range 2–4 mW cm^{-2}. All the features demonstrate that light, although not a thermodynamic parameter, mimics the thermal behaviour observed for the relaxation parameters.

In summary, we have investigated the photoinduced effects on the dielectric properties in the vicinity of the Sm-A–Sm-C$^*_A$ transition of a system comprising photoactive guest and non-photoactive host molecules. The studies show that in the Sm-C$^*_A$ phase, the molecular mode corresponding to the rotation of the molecules about their short axis can be seen in the planar configuration as well, although with a reduced dielectric strength. UV illumination is observed to bring out the presence of both the primary and secondary photo effects with substantial changes not only in the magnitude of the relaxation frequency of the molecular mode as well as the high-frequency mode (which, in the Sm-A phase, is the soft mode) but also in their temperature dependence.

Acknowledgment

We gratefully acknowledge the financial support by the Department of Science and Technology, New Delhi, under an SERC project (Grant No. 93357).

References

[1] Nair G G, Hegde G, Prasad S K, Lobo C V and Negi Y S 2006 *Phys. Rev.* E **73** 011712
[2] Chandani A D L, Gorecka E, Ouchi Y, Takezoe H and Fukuda A 1989 *Japan. J. Appl. Phys.* 2 **28** L1265
For reviews on the antiferroelectric and sub phases see Lagerwall S T 1999 *Ferroelectric and Antiferroelectric Liquid Crystals* (Germany: Wiley–VCH)
Musevic I, Blinc R and Zeks B 2000 *The Physics of Ferroelectric and Antiferroelectric Liquid Crystals* (Singapore: World Scientific)
[3] See e.g. Fukuda A, Takanishi Y, Isozaki T, Ishikawa K and Takezoe H 1994 *J. Mater. Chem.* **4** 997
[4] See, e.g. Rau H 1989 *Photochemistry and Photophysics* vol II, ed J F Rabek (Boca Raton, FL: CRC Press)
[5] Ikeda T and Tsutsumi O 1995 *Science* **268** 1873
[6] Coles H J, Walton H G, Guillon D and Poetti G 1993 *Liq. Cryst.* **15** 551
[7] Servaty S, Kremer F, Schonfeld A and Zentel R 1995 *Z. Phys. Chem.* **190** 73
[8] Legge C H and Mitchell G R 1992 *J. Phys. D: Appl. Phys.* **25** 492
[9] Sánchez C, Alcalá R, Hvilsted S and Ramanujam P S 2003 *J. Appl. Phys.* **93** 4454
[10] Tamaoki N 2001 *Adv. Mater.* **13** 1135
[11] Nair G G, Prasad S K and Yelamaggad C V 2000 *J. Appl. Phys.* **87** 2084
[12] Prasad S K and Nair G G 2001 *Adv. Mater.* **13** 40
Prasad S K, Nair G G and Hegde G 2005 *Adv. Mater.* **17** 2086
[13] Knobloch H, Orendi H, Buchel M, Seki T, Ito S and Knoll W 1995 *J. Appl. Phys.* **77** 481
[14] Blinov L M, Kozlovsky M V, Ozaki M, Skarp K and Yoshino K 1998 *J. Appl. Phys.* **84** 3860
[15] Eich M, Reck B, Ringsdorf H and Wendorff J H 1986 *Proc. SPIE* **682** 93
[16] Prasad S K, Sandhya K L, Shankar Rao D S and Negi Y S 2003 *Phys. Rev.* E **67** 051701
[17] Lemieux R P 2005 *Soft Matter* **1** 348
[18] Suzuki Y, Hagiwara T, Kawamura I, Okamura N, Kitazume T, Kakimoto M, Imai Y, Ouchi Y, Takezoe H and Fukuda A 1989 *Liq. Cryst.* **6** 167
[19] Moritake H, Ozaki M and Yoshino K 1993 *Japan. J. Appl. Phys.* 2 **32** L1432
[20] Havriliak S and Negami S 1966 *J. Polym. Sci.* C **14** 99

[21] Hiraoka K, Takezoe H and Fukuda A 1993 *Ferroelectrics* **147** 13
[22] Hiller S, Pikin S, Haase W, Goodby J and Nishiyama I 1994 *Japan. J. Appl. Phys.* 2 **33** L1170
[23] Buivydas M, Gouda F, Andersson G, Lagerwall S and Stebler B 1997 *Liq. Cryst.* **23** 723
[24] Panarin Y, Kalinovskaya O and Vij J 1998 *Liq. Cryst.* **25** 241
[25] Parry-Jones L A and Elston S J 2002 *J. Appl. Phys.* **92** 449
[26] See articles by Legrand Ch, Douali R, Dubois F and Nguyen H T 2003 *Relaxation Phenomena: Liquid Crystals, Magnetic Systems, Polymers, High-T_c Superconductors, Metallic Glasses* ed W Haase and S Wrobel (Berlin: Springer) pp 468–85
Wrobel S, Haase W, Fafara A and Marzec M 2003 *Relaxation Phenomena: Liquid Crystals, Magnetic Systems, Polymers, High-T_c Superconductors, Metallic Glasses* ed W Haase and S Wrobel (Berlin: Springer) pp 485–510
[27] Bibonne F, Parneix J P, Isaert N, Joly G, Nguyen H T, Bouchta A and Destrade C 1995 *Mol. Cryst. Liq. Cryst.* **263** 27
[28] Hegde G, Nair G G, Prasad S K and Yelamaggad C V 2005 *J. Appl. Phys.* **97** 093105
[29] Carlsson T, Zeks B, Filipic C and Levstik A 1990 *Phys. Rev.* A **42** 877
[30] Prasad S K, Khened S M, Raja V N, Chandrasekhar S and Shivakumar B 1993 *Ferroelectrics* **138** 37